


Kohn-Sham Density Functional Theory with Complex, Spin-Restricted Orbitals: Accessing a New Class of Densities without the Symmetry Dilemma

Joonho Lee,^{*} Luke W. Bertels,[†] David W. Small, and Martin Head-Gordon[‡]
College of Chemistry, University of California, Berkeley, California 94720, USA

 (Received 17 April 2019; published 10 September 2019)

We show that using complex, spin-restricted orbitals in Kohn-Sham (KS) density functional theory allows one to access a new class of densities that is not accessible by either spin-restricted (RKS) or spin-unrestricted (UKS) orbitals. We further show that the real part of a complex RKS (CRKS) density matrix can be nonidempotent when the imaginary part of the density matrix is not zero. Using CRKS orbitals shows significant improvements in the triplet-singlet gaps of a benchmark set, called TS12, for well-established, widely used density functionals. Moreover, it was shown that RKS and UKS yield qualitatively wrong charge densities and spin densities, respectively, leading to worse energetics. We demonstrate that representative modern density functionals show surprisingly no improvement even with a qualitatively more accurate density from CRKS orbitals. To this end, our work not only provides a way to escape the symmetry dilemma whenever there exists a CRKS solution, but also suggests a new route to design better approximate density functionals.

DOI: [10.1103/PhysRevLett.123.113001](https://doi.org/10.1103/PhysRevLett.123.113001)

Introduction.—Since its invention, Kohn-Sham density functional theory (KS-DFT) [1–3] has become the workhorse of *ab initio* nonrelativistic simulation of molecules and materials in condensed matter physics, materials science, chemistry, and other related disciplines. Given its computational efficiency and accuracy, it is well suited for a variety of applications including *ab initio* molecular dynamics simulations. Despite its popularity, two issues in practical KS-DFT remain unsolved: (i) strong correlation and (ii) self-interaction error [3,4]. In this Letter, we elucidate some aspects of KS-DFT regarding the first issue (i.e., strong correlation), which will help to further broaden the applicability of KS-DFT.

In KS-DFT, it is clear that for systems with antiferromagnetically coupled open-shell electrons, spin-unrestricted KS-DFT (UKS) behaves better than spin-restricted KS-DFT (RKS) at the expense of spin polarization [5–7]. For finite-sized systems, this spin polarization is a manifestation of the lack of strong (or static) correlation in a single-determinant wave function [8,9]. This is known as a symmetry dilemma in KS-DFT, so called because exact solutions for finite systems should not break spin symmetry yet the unphysical, spin-symmetry-broken approximate solutions often provide lower energies than symmetric approximate solutions.

As an attempt to address this symmetry dilemma, Perdew and co-workers proposed the use of “on-top” pair density [9,10], $\Pi(\mathbf{r})$, which is defined as

$$\Pi(\mathbf{r}) = \rho_{\alpha}(\mathbf{r})\rho_{\beta}(\mathbf{r}). \quad (1)$$

Instead of working with spin density variables $\rho_{\alpha}(\mathbf{r})$ and $\rho_{\beta}(\mathbf{r})$, the fundamental variables are now the charge density $\rho(\mathbf{r}) = \rho_{\alpha}(\mathbf{r}) + \rho_{\beta}(\mathbf{r})$ and the magnetization density $m(\mathbf{r})$, which is a function of $\rho(\mathbf{r})$ and $\Pi(\mathbf{r})$. One can accomplish the one-to-one mapping between $m(\mathbf{r})$ and $\Pi(\mathbf{r})$ following

$$m(\mathbf{r}) = \rho(\mathbf{r}) \left(1 - \frac{4\Pi(\mathbf{r})}{\rho(\mathbf{r})^2} \right)^{1/2}. \quad (2)$$

Evidently, inserting Eq. (1) into Eq. (2) yields a more familiar definition of the magnetization density, $m(\mathbf{r}) = \rho_{\alpha}(\mathbf{r}) - \rho_{\beta}(\mathbf{r})$. With $\rho(\mathbf{r})$ and $m(\mathbf{r})$, one can back out $\rho_{\alpha}(\mathbf{r})$ and $\rho_{\beta}(\mathbf{r})$ and these can be used to compute the exchange-correlation (XC) potential, $v_{xc}(\mathbf{r})$. This framework allows one to treat $m(\mathbf{r})$ as an auxiliary variable that is closely related to the on-top pair density. However, this does not remedy problems arising from evaluating $v_{xc}(\mathbf{r})$ with spin densities.

In this Letter, we describe a way to access a new class of charge and spin densities that is not accessible by spin polarization. This is achieved by breaking time-reversal symmetry and complex symmetry of the KS-DFT determinant [11–14]. We will refer to this symmetry breaking as “complex polarization.” For semilocal functionals, we show that this complex polarization does not pose any dilemma in obtaining charge and spin densities. We illustrate how this is achieved and demonstrate the numerical performance of popular semilocal functionals on chemical systems where complex polarization is *essential* to obtain correct charge and spin densities.

Theory.—We start from the KS-DFT Lagrangian [15],

$$\mathcal{L}[\mathbf{P}] = E_{\text{KS-DFT}}[\mathbf{P}] + \mu \left(\text{tr}(\mathbf{P}) - \frac{N}{2} \right) + \text{tr}[\mathbf{A}(\mathbf{P}^2 - \mathbf{P})] + \text{tr}[\mathbf{B}(\mathbf{P}^\dagger - \mathbf{P})], \quad (3)$$

where N is the number of electrons, \mathbf{P} is a one-particle density matrix (1PDM), μ , \mathbf{A} , and \mathbf{B} are Lagrange multipliers for constraining the trace, idempotency, and Hermiticity of \mathbf{P} , respectively. The idempotency of \mathbf{P} guarantees the noninteracting nature of the KS-DFT problem. For simplicity, we also assume that the computational basis is orthogonal.

These three constraints are naturally imposed by the definition of \mathbf{P} ,

$$\mathbf{P} = \mathbf{C}_{\text{occ}} \mathbf{C}_{\text{occ}}^\dagger, \quad (4)$$

where \mathbf{C}_{occ} is the occupied molecular orbital (MO) coefficient matrix. However, when minimizing Eq. (3) with respect to \mathbf{P} directly, it is necessary to consider these constraints explicitly or impose them through density matrix purification techniques [16]. We write \mathbf{P} in terms of its real and imaginary components,

$$\mathbf{P} = \mathbf{X} + i\mathbf{Y}. \quad (5)$$

We can then rewrite these constraints as follows: the trace condition leads to

$$\text{tr}(\mathbf{X}) = \frac{N}{2}, \quad (6)$$

$$\text{tr}(\mathbf{Y}) = 0, \quad (7)$$

the idempotency becomes

$$\mathbf{X} = \mathbf{X}^2 - \mathbf{Y}^2, \quad (8)$$

$$\mathbf{Y} = \mathbf{X}\mathbf{Y} + \mathbf{Y}\mathbf{X}, \quad (9)$$

and the Hermiticity yields

$$\mathbf{X} = \mathbf{X}^T, \quad (10)$$

$$\mathbf{Y} = -\mathbf{Y}^T. \quad (11)$$

Based on Eq. (11), we conclude that \mathbf{Y} is antisymmetric and therefore it automatically satisfies Eq. (7). This is an important observation since $\rho(\mathbf{r})$ is computed from \mathbf{P} following

$$\rho(\mathbf{r}) = 2 \sum_{\mu\nu} \eta_\mu(\mathbf{r}) \eta_\nu(\mathbf{r}) P_{\mu\nu}, \quad (12)$$

where $\eta_\mu(\mathbf{r})$ is a real-valued computational basis function. Since $\eta_\mu(\mathbf{r})\eta_\nu(\mathbf{r})$ is a symmetric tensor, an antisymmetric tensor \mathbf{Y} does not contribute to $\rho(\mathbf{r})$. In other words, it is equivalent to write $\rho(\mathbf{r}) = 2 \sum_{\mu\nu} \eta_\mu(\mathbf{r}) \eta_\nu(\mathbf{r}) X_{\mu\nu}$.

The key insight here is that by having nonzero \mathbf{Y} , the idempotency constraint on \mathbf{X} can be relaxed to Eqs. (8) and (9). In other words, \mathbf{X} does not have to satisfy $\mathbf{X} = \mathbf{X}^2$ as long as \mathbf{Y} is non-negligible. Such a density matrix \mathbf{P} with $\text{tr}(\mathbf{Y}^T \mathbf{Y}) \neq 0$ is referred to as a ‘‘fundamentally complex’’ density matrix. It is fundamentally complex in the sense that no unitary rotation of a real-valued MO coefficient matrix in the complex plane can represent a fundamentally complex density matrix [13]. Consequently, the use of fundamentally complex density matrices results in a broader (than RKS) class of densities, arising from a nonidempotent density matrix \mathbf{X} . It is not obvious whether lifting this idempotency constraint on \mathbf{X} would always yield a lower energy solution. In fact, the energy lowering turns out to be quite rare and singlet open-shell systems with high point group symmetry tend to exhibit this energy lowering.

For semilocal functionals, $E_{\text{KS-DFT}}$ depends only on \mathbf{X} and reads

$$E_{\text{KS-DFT}}[\mathbf{X}] = E_T[\mathbf{X}] + E_V[\rho(\mathbf{r})] + E_J[\rho(\mathbf{r}v)] + E_{\text{XC}}[\rho(\mathbf{r}), \nabla\rho(\mathbf{r}), \dots] + E_{nn}, \quad (13)$$

where the kinetic energy is defined as

$$E_T[\mathbf{X}] = 2\text{tr}(\mathbf{X}\mathbf{T}), \quad (14)$$

with the kinetic energy matrix \mathbf{T} in the computational basis ($T_{\mu\nu} = \langle \mu | -\frac{1}{2}\nabla^2 | \nu \rangle$), the nuclear-electron attraction energy is

$$E_V[\rho(\mathbf{r})] = -\sum_I Z_I \int_{\mathbf{r}} \frac{\rho(\mathbf{r})}{\|\mathbf{r} - \mathbf{R}_I\|_2}, \quad (15)$$

with I denoting the nuclei (or ions), the electron-electron repulsion energy reads

$$E_J[\rho(\mathbf{r})] = \frac{1}{2} \int_{\mathbf{r}_1} \int_{\mathbf{r}_2} \frac{\rho(\mathbf{r}_1)\rho(\mathbf{r}_2)}{\|\mathbf{r}_1 - \mathbf{r}_2\|_2}. \quad (16)$$

E_{XC} denotes the XC energy and E_{nn} is the nuclear-nuclear repulsion energy. We emphasize that as far as Eq. (13) is concerned there is no symmetry breaking associated with \mathbf{X} and ρ . Furthermore, no auxiliary variable is needed for energy evaluation.

Beyond permitting access to densities not describable by RKS and even UKS, one other point should be mentioned. Just as \mathbf{X} is nonidempotent, the CRKS determinant is inherently multiconfigurational (MC) as shown in Ref. [13]. A complex orbital ξ is, in terms of real η and

imaginary $\bar{\eta}$ orbitals, parametrized by θ : $\xi = \cos(\theta)\eta - i \sin(\theta)\bar{\eta}$. A two-electron closed-shell determinant made of a complex spatial orbital ξ_i follows

$$|\Psi\rangle = \mathcal{A}[\xi\xi(\alpha\beta)] = \mathcal{A}[(\Pi + \Omega)(\alpha\beta)], \quad (17)$$

where \mathcal{A} is the antisymmetrizer including a normalization factor, $\Pi = \cos^2(\theta)\eta\eta - \sin^2(\theta)\bar{\eta}\bar{\eta}$, and $\Omega = -i \sin(\theta) \cos(\theta)(\eta\bar{\eta} + \bar{\eta}\eta)$. These two spatial wave functions Π and Ω highlight the MC character of a CRKS single-determinant $|\Psi\rangle$. Π is a two-configuration wave function (lower energy) and Ω is an open-shell wave function (higher energy). The competition between energy-lowering via Π and an energy penalty through Ω determines whether an RKS electron pair complexifies to CRKS. In the η basis, the corresponding 2×2 matrix \mathbf{X} is

$$\mathbf{X} = \begin{bmatrix} \cos^2(\theta) & 0 \\ 0 & \sin^2(\theta) \end{bmatrix}. \quad (18)$$

$\theta = 0$ represents an RKS density matrix, whereas $\theta = \pi/4$ yields two half-occupied orbitals. Depending on θ , it is possible to obtain a nonidempotent \mathbf{X} . While the hidden MC form in the CRKS determinant is limited, its real 1PDM (for E_T) and its $\rho(\mathbf{r})$ (for E_J and E_V) can all be consistently evaluated using existing XC functionals. Thus CRKS can be viewed as a limited case of MC-DFT without the formal challenges [17–19] and practical double-counting problems [4,17,20–24] normally associated with that field.

Results.—We evaluate the numerical performance of RKS, UKS, and CRKS on the recently developed TS12 benchmark set [14]. This dataset contains the experimental singlet-triplet gaps of 12 atoms and molecules: C, NF, NH, NO⁻, O₂, O, PF, PH, S₂, S, Si, and SO. The ground states of these molecules are triplets. The lowest singlet states for each system are singlet biradicals and exhibit a spin-restricted Hartree-Fock (RHF) to complex RHF instability. This instability is driven by the underlying point group symmetry which gives rise to the degeneracy between the

highest occupied MO (HOMO) and the lowest unoccupied MO (LUMO).

The correct lowest singlet states of these systems should singly-occupy both HOMO and LUMO and thereby obtain charge and spin densities that obey the underlying point group symmetry. Even with the exact XC functional, RKS orbitals are qualitatively wrong in these cases as they doubly occupy the HOMO, breaking the point group symmetry of the system and leading to a broken-symmetry charge density. Since the exact XC functional yields not only exact energy but also exact charge density, accessing a different class of density matrix other than those from RKS orbitals is necessary. A similar phenomenon was first pointed out by Pople, Gill, and Handy in the context of spin polarization in open-shell systems [25]. Indeed, UKS can achieve these single occupations by breaking spin symmetry. However, we will show that spin polarization is not the way to access the right charge and spin densities in the systems in TS12.

We investigate a local density approximation (LDA) functional, SPW92 [26–29], two generalized gradient approximation (GGA) functionals, BLYP [30,31] and PBE [32], and four meta-GGA (MGGA) functionals, TPSS [33], SCAN [34], MN15-L [35], and B97M-V [36]. We used aug-cc-pVQZ basis set [37,38], and 99 and 590 points for radial and angular quadrature, respectively, as implemented in Q-Chem [39]. We only report KS-DFT solutions found to be locally stable based on stability analysis [40,41]. The triplet ground states are computed with UKS ($M_S = 1$) and we focus on the symmetry dilemma of the singlet states.

In Table I, we present the root-mean-square-deviation (RMSD) and mean-signed deviation (MSD) of the relatively old XC functionals SPW92, BLYP, PBE, and TPSS. Using RKS orbitals clearly overestimates the triplet-singlet gap (i.e., positive MSDs) as restricted orbitals cannot describe the open-shell nature of the lowest singlet state of these systems. Using UKS orbitals has the opposite problem. Namely, the gaps are all underestimated. This is due to the undesired mixing of the singlet and triplet states

TABLE I. The deviation (kcal/mol) with respect to experimental values in $\Delta E_{T-S}(= E_S - E_T)$ for 7 density functionals obtained with restricted, unrestricted, and complex, restricted orbitals. Note that MN15-L and B97M-V have no stable CRKS solutions for half of the data points (i.e., C, NF, NH, NO⁻, O₂, and O).

	SPW92	PBE	BLYP	TPSS	SCAN	MN15-L	B97M-V
				RKS			
MSD	10.85	13.09	9.94	13.85	19.50	10.64	11.82
RMSD	11.46	13.53	10.34	14.42	19.82	11.16	12.22
				UKS			
MSD	-13.70	-16.57	-17.61	-17.26	-16.24	-10.79	-13.69
RMSD	14.46	17.61	18.64	18.19	17.74	11.97	14.71
				CRKS			
MSD	-1.23	3.00	0.90	7.94	15.55	10.50	10.34
RMSD	2.19	3.41	1.91	8.63	16.39	11.00	11.15

TABLE II. The energy differences (kcal/mol) between CRKS and RKS solutions of O_2 (i.e., $\Delta E = \Delta E_{\text{CRKS}} - \Delta E_{\text{RKS}}$) for each component in Eq. (13). $\Delta E_{\text{Coul}} = \Delta E_J + \Delta E_V$, ΔE_X , and ΔE_C are the energy differences in classical Coulomb energy, exchange energy, and correlation energy, respectively.

	ΔE_T	ΔE_V	ΔE_J	ΔE_{Coul}	ΔE_X	ΔE_C	ΔE_{XC}
SPW92	12.89	-45.70	11.65	-34.05	7.88	0.20	8.09
PBE	10.69	-39.57	7.06	-32.51	12.13	-1.38	10.76
BLYP	9.96	-36.43	4.09	-32.33	13.05	-0.38	12.67
TPSS	5.95	-26.95	-2.28	-29.22	18.45	-1.65	16.80

(i.e., spin contamination). Since the triplet state is lower in energy, the resulting UKS $M_S = 0$ state energy is too low. Viewed differently, the UKS $M_S = 0$ state suffers from an unphysical (nonzero) net spin density. The use of CRKS orbitals improves both the MSD and RMSD by more than a factor of 5 in the case of SPW92, PBE, and BLYP. The improvement in TPSS is less impressive although it is still a factor of 2 improvement.

This significant improvement is simply due to obtaining ρ from a nonidempotent \mathbf{X} without spin polarization. Indeed, in all systems in TS12, the resulting \mathbf{X} has exactly two eigenvalues of 0.5 when obtained from these four XC functionals. These two eigenvalues represent the single occupancy of HOMO and LUMO, which is qualitatively correct for these systems. To understand what drives the energy lowering from RKS to CRKS, we decompose the energy difference between RKS and CRKS into individual energy contributions. We present this energy decomposition for O_2 in Table II. The qualitative behavior discussed here holds for other systems as well. All four XC functionals show an increase in the kinetic energy as well as the XC energy. The increase in the XC energy is driven by the increase in the exchange energy. The correlation energy shows only a small change. The RKS to CRKS instability is driven by the classical Coulomb energy. In particular, a significant energy lowering in the electron-nuclear attraction energy is the driving force of this instability in all systems in the TS12 set. Such an increase in kinetic energy accompanied by a decrease in electron-nuclear attraction reflects the virial theorem, which must hold for variational approaches such as KS-DFT.

The results for the more modern MGGA functionals SCAN, MN15-L, and B97M-V, are also presented in Table I. The RKS and UKS results are qualitatively similar to what was observed in the above four functionals. Namely, the overestimation in gaps was observed with RKS while the underestimation in gaps was observed with UKS. SCAN with RKS orbitals shows a particularly poor behavior compared to all the other functionals examined in this work. SCAN becomes comparable to other functionals when used with UKS orbitals. The CRKS results with these three modern functionals are rather surprising due to a qualitatively different behavior from that of the four

functionals discussed before. The use of CRKS orbitals for these functionals does not improve the quantitative energetics. Furthermore, MN15-L and B97M-V exhibit no stable CRKS solutions for C, NF, NH, NO^- , O_2 , and O. Additionally, MN15-L shows occupation numbers of (0.61, 0.39) and (0.78, 0.22) for PF and PH, respectively. The poor performance of these modern MGGA functionals with CRKS orbitals suggests that data such as the TS12 set may be useful for XC functional development.

Lastly, we present density plots to compare the qualitative differences between densities from RKS and CRKS orbitals. As mentioned throughout this Letter, RKS orbitals break the point group spatial symmetry of systems in the TS12 set whereas CRKS orbitals preserve the symmetry [42]. The symmetry breaking at the orbital level results in the symmetry breaking in ρ . We shall illustrate this point by looking at ρ represented on a real-space grid.

In Fig. 1, we present the real-space density of O_2 computed with BLYP. The discussion also applies to other systems in the TS12 set and real-space densities are qualitatively similar across different XC functionals. O_2 is cylindrically symmetric around its interatomic axis. Therefore, qualitatively correct density should exhibit this

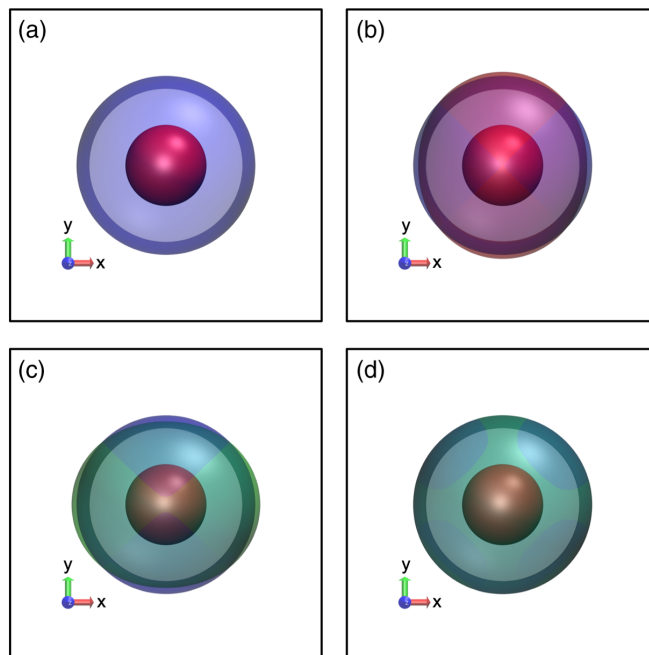


FIG. 1. Density $[\rho(\mathbf{r})]$ represented on a real-space grid for O_2 computed with the BLYP XC functional. O_2 is aligned along the bond axis (z axis) so that we can inspect the cylindrical symmetry of density. (a) CRKS density (blue), (b) RKS (red) density superimposed on CRKS density (blue), (c) UKS (green) two times α -spin density $[2\rho_\alpha(\mathbf{r})]$ superimposed on CRKS density (blue), and (d) UKS (green) charge-density superimposed on CRKS density (blue). The factor of 2 in (c) is to account for the difference between normalization factors of charge and spin densities. Every plot is based on an isosurface value of 0.08 au. The z axis is pointing out of the page.

symmetry. This is found to be true with the CRKS density in Fig. 1(a). However, in Fig. 1(b), the RKS density is elongated along the y axis and overall not cylindrically symmetric. This is due to the spatial symmetry breaking caused by doubly occupying the HOMO which mixes two low-lying singlet states, $^1\Delta_g$ and $^1\Sigma_g^+$ [13]. The UKS α -spin density breaks cylindrical symmetry to a smaller extent than does RKS and is elongated along the x axis. The UKS charge density (i.e., the sum of α and β density) is only x - y symmetric and breaks the cylindrical symmetry. The x - y symmetry is because the UKS β -spin density is rotated 90° from the α density (i.e., elongated along the y axis).

The qualitatively improved UKS charge density (compared to the RKS one) is attractive though it is still qualitatively wrong. The on-top pair density interpretation provides a way to understand the spin-symmetry breaking in this case, but there is no quantitative benefit. The resulting energetics from the UKS spin densities are far from chemical accuracy (1 kcal/mol) as it is clear in Tables I and II. In particular, the improved UKS charge density (compared to RKS) comes at the expense of significant net spin density, which is physically incorrect. In contrast to this, we observe a qualitatively correct charge density (and also zero net spin density) with the CRKS determinant. At the same time, the resulting CRKS triplet-singlet gaps are improved as shown in Table I.

Conclusions.—In this Letter, we showed that it is possible to access a different class of densities that is not possible to obtain within either RKS or UKS. This is achieved by using CRKS to obtain the density. Although the CRKS determinant breaks time-reversal symmetry and complex symmetry, the resulting densities do not exhibit the spatial and spin symmetry breaking associated with RKS and UKS. Furthermore, based on the triplet-singlet test set (TS12), we showed that the CRKS charge densities follow the point group symmetry while RKS does not. This allows CRKS to improve the quantitative accuracy of some XC functionals by a factor of 5. We also showed that the UKS charge density is qualitatively incorrect and the resulting energies are far from chemical accuracy due to spin contamination. Lastly, we note that modern MGGA functionals (SCAN, MN15-L, and B97M-V) do not show any significant improvements even when correct densities from CRKS are used. Even with the exact XC functional, one needs a CRKS determinant to obtain qualitatively correct charge and spin densities for the systems considered here. This Letter suggests that these modern functionals might lack some aspects of the exact XC functional. We hope that our study provides a new class of data that can be used to assess, and possibly inform the design of new approximate XC functionals. The key benefit is a route to escape the symmetry dilemma whenever complex polarization is relevant.

The Supplemental Material for this work is available online [43]. This research was supported by the Director,

Office of Science, Office of Basic Energy Sciences, of the U.S. Department of Energy under Contract No. DE-AC02-05CH11231. We thank Fionn Malone, Yuezhi Mao, and Narbe Mardirossian for helpful comments. J.L. thanks Soojin Lee for consistent encouragement.

Note added in the proof.—The discussions presented above are for the finite basis simulation of Kohn-Sham equations. Recently, we became aware of the Harriman construction [45] which asserts the existence of a real, spin-restricted determinant for any density at the continuum limit.

*linusjoonho@gmail.com

†lwbertels@gmail.com

‡mhg@cchem.berkeley.edu

- [1] W. Kohn and L. J. Sham, *Phys. Rev.* **140**, A1133 (1965).
- [2] R. G. Parr and W. Yang, *Density-Functional Theory of Atoms and Molecules*, International Series of Monographs on Chemistry (Oxford University Press, Oxford, UK, 1994).
- [3] N. Mardirossian and M. Head-Gordon, *Mol. Phys.* **115**, 2315 (2017).
- [4] A. J. Cohen, P. Mori-Sánchez, and W. Yang, *Chem. Rev.* **112**, 289 (2012).
- [5] O. Gunnarsson and B. I. Lundqvist, *Phys. Rev. B* **13**, 4274 (1976).
- [6] J. M. Seminario, *Int. J. Quantum Chem.* **52**, 655 (1994).
- [7] E. R. Davidson, *Int. J. Quantum Chem.* **69**, 241 (1998).
- [8] P. Lykos and G. W. Pratt, *Rev. Mod. Phys.* **35**, 496 (1963).
- [9] J. P. Perdew, A. Savin, and K. Burke, *Phys. Rev. A* **51**, 4531 (1995).
- [10] J. P. Perdew, M. Ernzerhof, K. Burke, and A. Savin, *Int. J. Quantum Chem.* **61**, 197 (1997).
- [11] H. Fukutome, *Int. J. Quantum Chem.* **20**, 955 (1981).
- [12] J. L. Stuber and J. Paldus, *Fundamental World of Quantum Chemistry: A Tribute to the Memory of Per-Olov Löwdin*, edited by E. J. Brändas and E. S. Kryachko (Springer, New York, 2003), Vol. 1, pp. 67–139.
- [13] D. W. Small, E. J. Sundstrom, and M. Head-Gordon, *J. Chem. Phys.* **142**, 024104 (2015).
- [14] J. Lee and M. Head-Gordon, *J. Chem. Phys.* **150**, 244106 (2019).
- [15] A. G. Taube, *J. Chem. Phys.* **133**, 151102 (2010).
- [16] J. Kussmann, M. Beer, and C. Ochsenfeld, *Comput. Mol. Sci.* **3**, 614 (2013).
- [17] B. Miehlich, H. Stoll, and A. Savin, *Mol. Phys.* **91**, 527 (1997).
- [18] J. Gräfenstein, E. Kraka, and D. Cremer, *Chem. Phys. Lett.* **288**, 593 (1998).
- [19] Y. Kurzweil, K. V. Lawler, and M. Head-Gordon, *Mol. Phys.* **107**, 2103 (2009).
- [20] S. Gusarov, P.-Å. Malmqvist, and R. Lindh, *Mol. Phys.* **102**, 2207 (2004).
- [21] Y. G. Khait and M. R. Hoffmann, *J. Chem. Phys.* **120**, 5005 (2004).
- [22] G. Li Manni, R. K. Carlson, S. Luo, D. Ma, J. Olsen, D. G. Truhlar, and L. Gagliardi, *J. Chem. Theory Comput.* **10**, 3669 (2014).

- [23] S. Veeraraghavan and D. A. Mazziotti, *Phys. Rev. A* **89**, 010502(R) (2014).
- [24] S. Veeraraghavan and D. A. Mazziotti, *J. Chem. Phys.* **140**, 124106 (2014).
- [25] J. A. Pople, P. M. Gill, and N. C. Handy, *Int. J. Quantum Chem.* **56**, 303 (1995).
- [26] P. Hohenberg and W. Kohn, *Phys. Rev.* **136**, B864 (1964).
- [27] W. Kohn and L. J. Sham, *Phys. Rev.* **140**, A1133 (1965).
- [28] J. C. Slater, *The Self-consistent Field for Molecules and Solids. Quantum Theory of Molecules and Solids* (McGraw-Hill, New York, USA, 1963), Vol. 4.
- [29] J. P. Perdew and Y. Wang, *Phys. Rev. B* **45**, 13244 (1992).
- [30] A. D. Becke, *Phys. Rev. A* **38**, 3098 (1988).
- [31] C. Lee, W. Yang, and R. G. Parr, *Phys. Rev. B* **37**, 785 (1988).
- [32] J. P. Perdew, K. Burke, and M. Ernzerhof, *Phys. Rev. Lett.* **77**, 3865 (1996).
- [33] J. Tao, J. P. Perdew, V. N. Staroverov, and G. E. Scuseria, *Phys. Rev. Lett.* **91**, 146401 (2003).
- [34] J. Sun, A. Ruzsinszky, and J. P. Perdew, *Phys. Rev. Lett.* **115**, 036402 (2015).
- [35] S. Y. Haoyu, X. He, and D. G. Truhlar, *J. Chem. Theory Comput.* **12**, 1280 (2016).
- [36] N. Mardirossian and M. Head-Gordon, *J. Chem. Phys.* **142**, 074111 (2015).
- [37] T. H. Dunning, *J. Chem. Phys.* **90**, 1007 (1989).
- [38] R. A. Kendall, T. H. Dunning, and R. J. Harrison, *J. Chem. Phys.* **96**, 6796 (1992).
- [39] Y. Shao *et al.*, *Mol. Phys.* **113**, 184 (2015).
- [40] R. Bauernschmitt and R. Ahlrichs, *J. Chem. Phys.* **104**, 9047 (1996).
- [41] S. M. Sharada, D. Stück, E. J. Sundstrom, A. T. Bell, and M. Head-Gordon, *Mol. Phys.* **113**, 1802 (2015).
- [42] It turns out that for the atoms in TS12 (i.e., C, O, S, and Si) some subtlety arises. The singlet ground state of these atoms is fivefold degenerate (¹D). The CRKS density is not spherically symmetric since it cannot describe this ground state degeneracy. However, we were able to obtain a nonsymmetric density from exact wave function calculations (full configuration interaction) that is very similar to the CRKS density. If densities from these five degenerate solutions are averaged with equal weights, one obtains a spherically symmetric density. We conclude that the CRKS density is still qualitatively correct up to the ground state degeneracy.
- [43] See Supplemental Material at <http://link.aps.org/supplemental/10.1103/PhysRevLett.123.113001> for the raw data for TS12 (Tables I, II) along with high-accuracy theoretical benchmarks, which includes Refs. [14] and [44].
- [44] J. E. Smith, B. Mussard, A. A. Holmes, and S. Sharma, *J. Chem. Theory Comput.* **13**, 5468 (2017).
- [45] J. E. Harriman, *Phys. Rev. A* **24**, 680 (1981).